Heterogeneous Nucleation of Dicalcium Phosphate Dihydrate on Modified Silica Surfaces

Carrie Miller[1], Ljepša Komunjer[2], Vladimir Hlady[1]*

[1]Departments of Bioengineering and Materials Science and Engineering, University of Utah, Salt Lake City, Utah, USA
[2]Departement de Génie des Procédés Industriels, Université de Technologie de Compiègne, Compiègne, France
Submitted to:
Medicinski Vjesnik, Dr. Helga Füredi-Milhofer Festschrift
Correspondence:
Prof. Vladimir Hlady
Department of Bioengineering, University of Utah, Salt Lake City, Utah, USA
Email : vladimir.hlady@utah.edu

Heterogeneous nucleation of dicalcium phosphate dihydrate, $CaHPO_4 \cdot 2H_2O$ (DCPD) was studied on untreated planar fused silica and on three modified silica surfaces: octadecylsilyl (OTS) modified silica, human serum albumin treated OTS silica, and UV-oxidized 3-mercaptopropyltriethoxysilyl (MTS) modified silica. The supersaturation ratio of calcium and phosphate solution with respect to DCPD was kept below ~10. The nucleated crystals were observed 24 hours and one week after initial contact between supersaturated solutions and substrate surfaces using bright field and reflectance interference contrast microscopy. No DCPD crystals nucleated on albumin-treated OTS-silica. Majority of the DCDP crystals formed on the other modified silica surfaces appeared to be morphologically similar irrespective of the nature of nucleating substrate. Reflectance interference contrast microscopy provided a proof that the majority of the crystals on these substrates do not develop an extended contact with the substrate surface. The images showed that the most extended contact planes were between the DCPD crystals and MTS modified silica surface. The crystals nucleated on OTS-treated and untreated silica surfaces showed only few or none well-developed contact planes.

Keywords: Calcium phosphate; Dicalcium phosphate dihydrate; Heterogeneous nucleation theory; Microscopy – instrumentation, methods; Microscopy – reflectance interference contrast

INTRODUCTION

When crystal is to be formed from supersaturated liquid mother phase, the first step of the process is the formation of nucleus of this new phase. For thermodynamic reasons the nucleation process is accompanied by energetic barrier related to the formation of the interface between the new-born nucleus and the liquid mother phase. This energetic cost is dependent on the properties of the substance to crystallize and of the solvent used but also on the mechanism by which the nucleus is formed. The main distinction is between the mechanism of nucleation in the bulk of solution and nucleation on a substrate. The latter mechanism is known as heterogeneous nucleation (HEN) while nucleation in the bulk solution is referred to as homogeneous nucleation (HON). Although HEN is of great practical importance in many fields, its theoretical basis is not so often described in the literature compared to the HON. We shall therefore briefly present some basic features of the classical nucleation theories (for details see [1-3]) and illustrate them with the heterogeneous nucleation of dicalcium phosphate dihydrate, $CaHPO_4 \cdot 2H_2O$ (DCPD), on planar modified silica surfaces.

The nucleation and growth of poorly soluble calcium salts have been a long established interest of Dr. Füredi-Milhofer and the Laboratory for Precipitation Processes at Ruđer Bošković Institute. Two of us (Lj.K. and V.H.) have worked with Dr. Füredi-Milhofer on interactions of calcium hydroxyapatite (CaHA) crystals with human albumin [4], water structure within CaHA [5], formation of amorphous calcium phosphate (ACP) in presence of gelatin [6], as well as on precipitation of calcium oxalates [7], before turning to other research topics.

Dicalcium phosphate dihydrate is one of the sparingly soluble calcium phosphate salts which also include those involved in bone and dentin mineralization, i.e. calcium hydroxyapatite, octacalcium phosphate (OCP) and ACP. It has been shown that DCPD forms from tooth mineral under caries-like conditions [8]. It has also been proposed as a precursor to CaHA formation in bone, calculus, and in urinary calculi [9]. The solubility product of DCPD, K_{spDCPD} is 1.87×10^{-7} $(mol/L)^2$ [10]. The choice of using DCPD in the present study was related to the size of the DCPD crystals. Unlike CaHA, OCP or ACP, the crystals of DCPD nucleate on solid supports and grow to a size large enough to directly observe the growth

rate and the contact area between the solid support and the crystal using optical microscopy.

Supersaturation and Nucleation

For nucleation to occur, it is necessary to bring the solution concentration, c, to a value higher than the equilibrium concentration at saturation, c_s. In practice, this can be achieved either by cooling a saturated solution, by evaporation of the solvent or by mixing of two solutions containing ionic species forming slightly soluble solid substance. In all cases the difference of chemical potential per solute molecule, $\Delta\mu$, between supersaturated and saturated solution is given by:

$$\Delta\mu = k_B T \ln(c/c_s) = 2\gamma v/r^* \qquad (1)$$

where k_B is the Boltzmann constant, T is the absolute temperature, γ is the free energy of the interface nucleus/solution, v is the volume of a molecule in the nucleus and r^* is the radius of the critical nucleus with supposed spherical shape.

Eq. 1, known as Thomson-Gibbs equation, shows that for each solution concentration exists one size of nucleus, r^*, for which a labile equilibrium between crystal and solution can be established. One should note that the solubility of a substance, i.e. the concentration, c_s, corresponds to the equilibrium between solution and crystal of infinite size (then $c = c_s$ and $\Delta\mu = 0$

Activation Free Energy of Nucleation

If the mother phase is a homogeneous solution, the free energy barrier, ΔG, for the formation of a solid nucleus of i molecules is:

$$\Delta G = -i\Delta\mu + A_1\gamma_1 + A_2\gamma_2 + \dots, \qquad (2)$$

where $A_1, A_2,\dots$ represent the surface area of different crystal faces with corresponding surface energies $\gamma_1, \gamma_2, \dots$ of the nucleus. If the crystal reveals only one type of face, A, with surface energy γ, Eq. 2 reduces to:

$$\Delta G = -i\Delta\mu + A\gamma \qquad (3).$$

The first term of Eq. 3 represents the work gained by the association of i molecules which form the nucleus while the second term represents the energy cost associated with the creation of its surface. If the nucleus is spherical in shape with radius r, we have:

$$i = 4\pi r^3/3v$$
and
$$A = 4\pi r^2 \qquad (4).$$

By introducing Eq. 4 into Eq. 3 one can trace the variation of ΔG with nucleus dimension. When equilibrium is reached, i.e. when $d\Delta G/dr = 0$, the nucleus is said to achieve critical size at which the probability for the nucleus to dissociate is equal to

the probability to grow into a macroscopic crystal:

$$r^* = 2\gamma v/\Delta\mu \qquad (5).$$

By inserting Eq. 5 into Eqs. 3 and 4 one obtains the activation energy for nucleation:

$$\Delta G^* = 16\pi\gamma^3 v^2/3(\Delta\mu)^2 \qquad (6)$$

or

$$\Delta G^* = 4\pi r^{*2}\gamma/3 \qquad (7).$$

Numerical factor $16\pi/3$ in Eq. 6 is related to the spherical geometry of the nucleus; it changes with shape: for example, it becomes 32 for cube of edge length $2r$. From Eq. 6 one can see that high supersaturation will favour nucleation by lowering the energetic barrier ΔG^* (v and γ depend on the system).

In practice it is quite difficult to obtain the solid phase from bulk solution by the mechanism of homogeneous nucleation because heterogeneous nucleation on substrates (such as foreign particles, vessel walls or agitation device, etc.) often takes place before high supersaturation necessary for HON is achieved. The key property is then the *wetting* of the substance to crystallize. For convenience we shall consider the simple case of spherical cap crystal nucleating on flat solid substrate such as shown in Figure 1, while other geometries are treated in the literature [1,2]. Three interfacial free energies are to be considered in this case: the one between solid support and liquid mother phase, γ_{sl}, the one between nucleus and liquid mother phase, γ_{nl}, and the one between nucleus and support, γ_{sn}, so that total free energy change is:

$$\Delta G_{HEN} = -i\Delta\mu + A_{nl}\gamma_{nl} + A_{sn}\gamma_{sn} - A_{sl}\gamma_{sl} \qquad (8).$$

where the subscripts $_{nl, sl,}$ and $_{sn}$ refer to the parameters related to nucleus-liquid, substrate-liquid and nucleus- substrate interfaces, respectively.

With the well-known Young equation relating the three interfacial energies to the contact angle α of a spherical cap:

$$\gamma_{sl} = \gamma_{sn} + \gamma_{nl}\cos\alpha \qquad (9)$$

and using some geometry one finds the free energy change for a cap shaped nucleus formed by HEN:

$$\Delta G_{HEN} = -(4\pi r^3/3v)(2 - 3\cos\alpha + \cos^3\alpha)\,\Delta\mu/4 + 4\pi r^2\gamma_{nl}$$
$$(1 - \cos\alpha)/2 - 4\pi r^2\gamma_{nl}\cos\alpha(1 - \cos^2\alpha)/4 \qquad (10).$$

The equilibrium condition ($d\Delta G_{HEN}/dr = 0$) leads to the Thomson-Gibbs equation:

$$r^*_{HEN} = 2\gamma_{nl}v/\Delta\mu \qquad (11).$$

By introducing Eq. 11 into Eq. 10 and taking in account Eq. 7 one can compare the activation energy for HEN, ΔG^*_{HEN} with the corresponding energy for HON, ΔG^*:

$$\Delta G^*_{HEN}/\Delta G^* = 1/2 - (3/4)\cos\alpha + (1/4)\cos^3\alpha \qquad (12).$$

TABLE 1.
Contact angle and the corresponding ratio of critical activation energies for HEN and HON.
TABLICA 1.
Kontaktni kut i odgovarajući omjer kritične energije aktivacije za HEN i HON.

α (in degrees) α (u stupnjevima)	180	135	90	60	30	0
$\Delta G^*_{het}/\Delta G^*$	1	0.94	0.5	0.156	0.013	0

FIGURE 1.
Schematic presentation of a spherical crystal deposited on a planar solid substrate and
the corresponding interfacial energies and areas.
SLIKA 1.
Shematski prikaz sferoidnoga kristala na planarnom čvrstom supstratu i odgovarajuće međupovršinske energije i područja.
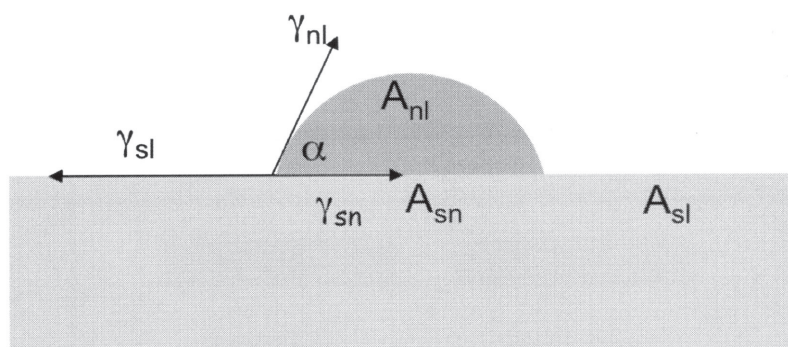
By inspecting the right hand side term of Eq. 12 one can see that for all values of α (except for $\alpha = 180°$) this term is smaller than 1 while for $\alpha = 0°$ the activation energy barrier ΔG^*_{HEN} disappears. This last particular case corresponds to the perfect wetting of the support by the substance to nucleate. For these reasons one can affirm that the presence of any solid support very likely facilitates the nucleation of crystals from solution: in case of perfect wetting i.e. $\alpha = 0°$ the barrier for nucleation vanishes completely, while for partial wetting ($0° < \alpha < 180°$) the barrier is lowered to the extent depending on the value of the contact angle. Only supports on which the contact angle is 180° have no influence on nucleation. Some more data concerning different wetting properties can be found in Table 1.

One should keep in mind that the determination of the "contact angle" between nucleating crystal and solid support is not an easy thing to do experimentally. Nonetheless, by examining the crystals grown on different substrates one can show that the large area of contact between the crystal and solid support indicates high wetting, while small area indicates lower wetting. Such an approach has been adopted here to illustrate the difference in heterogeneous nucleation of DPCD on several different silica substrates.

EXPERIMENTAL

The silica plates were cut from fused silica microscope slides (ESCO, Oak Ridge) to the size of 1 cm by 2 cm. The plates were cleaned with "piranha" solution (30 mL

H_2O_2 (30%) + 90 mL H_2SO_4) to remove all organic matter from surfaces and then rinsed with water 3 - 4 times. The cleaned plates were the placed in an 110°C vacuum overnight to completely dry them before deposition of the monolayers of octadecyltrichloro silane (OTS), human serum albumin (HSA), or 3-mercaptopropyltriethoxy silane (MTS).

OTS-treated silica. The cleaned silica was modified with octadecylsilyl groups (OTS) using the 0.2 wt% octadecyltrichloro silane solution in dry bicyclohexyl for 18 hours [11]. The OTS modified plates were washed with chloroform, then water and finally dried in a stream of nitrogen gas. The OTS plates were characterized by measuring water contact angles (~107°) to make sure the reaction had completed.

HSA-coated OTS-treated Silica. HSA-coated plate was prepared by incubating an OTS-modified plate in 0.1 mg/mL HSA in 0.15 M NaCl for two hours. The plates were then transferred to a 0.15 M NaCl bath for fifteen minutes. This rinsing step was then repeated. The wet HSA-treated OTS plates were immediately used in DCPD nucleation studies.

MTS-treated silica. A 2 vol% MTS solution in trichlorethylene (TCE) was used to treat cleaned silica plates overnight. The next day, the plates were washed with TCE, acetone, and ethanol. They were then dried under a stream of nitrogen gas and placed below an UV source. The UV source was set to expose the samples at 15.0 mW/cm² for five minutes. The

FIGURE 2.
Geometry of DCPD nucleation and growth experiments. [Ca++]tot, [PO4--]tot and [NaCl] mixture is placed in two neighbouring wells of a 96-wells polystyrene plate; completely filled wells are covered by a silica plate.
SLIKA 2.
Geometrija eksperimenta za nukleaciju i rast DCPD. Smjesa $[Ca^{++}]_{tot}$, $[PO_4^{--}]_{tot}$ i [NaCl] smještena je između dvije susjedne udubine na polistirenskoj ploči s 96 utora; otopinom ispunjene udubine pokrivene su s pločicom silike.
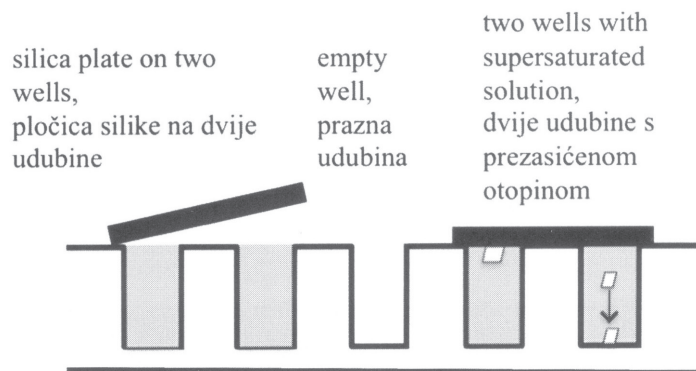

FIGURE 3.
a) Schematics of RICM: interference fringes are created by superposition of the light reflected by the object (DCPD crystal) and by the reference surface (silica substrate). b) Comparison between bright field (left) and RICM (right) images of a DCPD crystal grown on MTS-treated silica substrate. In the RICM image the dark area on the left side of the fringes corresponds to the contact plane (zero fringe order, m = 0) between the crystal and the substrate.
SLIKA 3.
a) Shematski prikaz RICM: interferencijski uzorak stvoren superpozicijom reflektiranog svjetla s objekta (kristal DCPD) i referentne površine (silika). b) Usporedba između slika DCPD kristala koji je izrastao na MTS-modificiranoj siliki, dobivenih pomoću obične mikroskopije (lijevo) i RICM (desno). Na RICM slici tamno polje na lijevoj strani ruba odgovara kontaktnom kutu plohe (nulti interferencijski uzorak, m = 0) između kristala i supstrata.
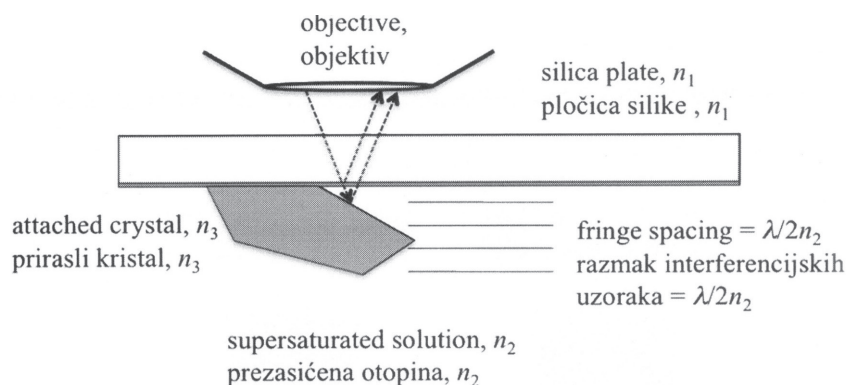
a)
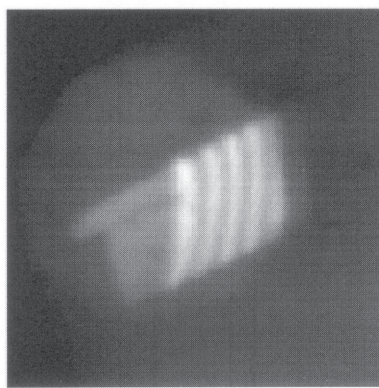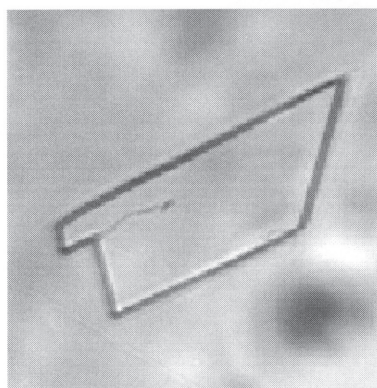
b)

treatment oxidized the surface thiol groups into the negatively charged sulfonate groups [12].

DCPD nucleation experiments. Analytical grade chemicals and double distilled water were used. The stock solutions of 0.2 M $CaCl_2$, 1.0 M NaCl, and 0.2 M Na_2HPO_4 were filtered through a 0.65 μm filter, diluted prior to mixing and the pH value of the phosphate solution was adjusted to a pH 5 by adding a small amount of HCl. The aliquots of the solutions were pipetted into the two neighbouring wells of a 96-wells polystyrene plate filling the wells completely to achieve predetermined final calcium and phosphate concentrations and thus the desired supersaturation. The surrounding wells were kept empty to prevent contamination.

Each silica plate was placed over the two neighbouring wells (Figure 2). Water was placed into the distant perimeter wells to maintain local humidity and alleviate evaporation. The 96-wells polystyrene plate was covered with a plastic cover and sealed to further prevent evaporation. Each 96-wells polystyrene plate was placed in a saturated humidity box and kept at room temperature. An upright Nikon microscope was adjusted to produce either a bright field or reflectance interference contrast images as to observe the crystals that had nucleated on the surfaces of silica plates in contact with the solution. Digitized images of the crystals were taken twenty-four hours and one week after the solutions and substrates were brought into contact with each other.

Reflectance Interference Contrast Microscopy. The principle of RICM is shown in Figure 3 and is described in details elsewhere [13,14]. Briefly, the interference fringes are created by constructive or destructive interference pattern formed by the superposition of the light reflected by the object (crystal) and by the reference surface (here: silica substrate) (Fig 3a). The vertical distance, d, between fringes is: $d = m\lambda/2n_2$, where m is the fringe order number, n_2 is the refractive index of the buffer medium, and λ is the wavelength of the monochromatic light, here ~450 nm. Thus, in aqueous solution the distance between each dark fringe corresponds to a vertical distance of 169 nm. The zero fringe order ($m = 0$) indicates the contact area between the crystal and the silica plate. The comparison between the bright field and RICM images of one surface-adherent DCPD crystal in shown in Fig 3b. By measuring the light intensity of the fringes in the RICM image (Fig 3b, bottom), one can analyze the crystal-silica plate contact region and also re-construct the 3D shape of the crystal in the proximity of the silica surface, none of which is possible using bright field optical microscopy image (Fig 3b, top). The RICM implementation on the Nikon microscope used in this study required that the field iris diaphragm of the incident light is almost closed. One can see the octagonal shape of the field iris in Fig 3b, bottom, as the dark region around the crystal.

RESULTS AND DISCUSSION

DCPD crystals were grown at pH 5, at room temperature, with NaCl concentration of 0.15 M, and in the $[Ca^{++}]_{tot}$ and $[PO_4^-]_{tot}$ concentration range from 0.02 to 0.035 M,

corresponding to the supersaturation ratios up to ~10 ([1*]). DCPD crystals did not nucleate on HSA-coated OTS-treated silica in this concentration range. Figures 4 – 6 show the DPCD crystals grown after 24 hours on other three substrates: untreated silica, OTS-treated silica and MTS-treated silica substrates, respectively. For each pair of $[Ca^{++}]_{tot}$ and $[PO_4^-]_{tot}$ concentrations the upper panel shows the bright field image and lower panel the corresponding RICM image. Comparison of the bright field images for the other three substrates showed that DCPD crystal morphology did not significantly differ between the three nucleating substrates: majority of the crystals were single crystals ~ 100 – 200 μm wide and up to 500 - 800 μm long. Very few crystals were found on the bottom of the wells, indicating that the DCPD crystals nucleated predominantly by heterogeneous nucleation on silica. Very few crystals were found attached to the polystyrene well walls. After seven days of growth some bigger crystals detached from untreated silica and OTS-treated silica and were found on the bottom of the wells. When solutions with supersaturation ratios higher than 10 were used, multiple crystals nucleate on the same substrate location (data not shown).

It was unexpected that the gross DCPD crystal morphology did not depend on the surface characteristics of the nucleating substrates ([2**]). How could OTS-treated silica, a non-polar, low surface energy substrate with water contact angles ~107°, and untreated silica and UV-oxidized MTS-treated silica, each negatively charged, higher surface energy substrates with water contact angles of ~ 0° – 5° and 20°, respectively, nucleate morphologically similar DCPD crystals? The answer to this question was found by the inspection of the corresponding RICM images of the attached crystals. Namely, RICM images revealed the "footprint" of each attached crystal and the actual contact region between the crystal and the support. Although the RICM technique was able to image only a part of the crystals due to the limited field of view, the RICM inspection of the attached crystals indicated that only in the case of negatively charged MTS-treated silica surface the nucleation and growth resulted with larger DCPD crystal planes in contact with the substrates (Fig 6). Majority of the crystals grown on MTS-treated silica showed a well-developed attachment plane between the substrate and the DCPD crystal. Because the first RICM observation was taken 24 hours after the initial mixing of the solution and contact with the substrate, it is not known whether the growth of the attachment plane preceded the 3-D growth of crystal into the solution or the attachment area grew in parallel with the 3-D growth of the crystal.

In contrast to MTS-modified silica, DCPD crystals attached to OTS-treated silica surfaces showed very few well-developed contact planes in RICM images (Fig 5). It seems plausible that

1 * Calculated using the following data: - dissociation constants of phosphoric acid : $K_1 = 6.1 \cdot 10^{-3}$ M, $K_2 = 6.6 \cdot 10^{-8}$ M, and $K_3 = 6.6 \cdot 10^{-13}$ M, - association constant of calcium phosphate complexes : $K_{(CaH_2PO_4^+)} = 681$ M^{-1}, $K_{(CaHPO_4)} = 0.32$ M^{-1}, and $K_{(CaPO_4^-)} = 3.64 \cdot 10^6$ M^{-1}, and - solubility product of DPCD : K_{spDCPD} is 1.87 x 10^{-7} $(mol/L)^2$.

2 ** The amount of nucleating DCPD might have been different at different substrates but this information was not evaluated in the present study.

FIGURE 4.
DPCD crystals grown after 24 hours on clean silica from solutions of [Ca++]tot and [PO4--]tot as indicated. For each pair of [Ca++]tot and [PO4--]tot concentrations the upper panel shows the bright field image and the lower panel the corresponding RICM image.
SLIKA 4.
Kristal DCPD na čistoj siliki nakon 24h rasta iz otopina $[Ca^{++}]_{tot}$ i $[PO_4^{--}]_{tot}$ kako je naznačeno. Za svaki par koncentracija $[Ca^{++}]_{tot}$ i $[PO_4^{--}]_{tot}$ gornja slika je dobivena pomoću obične mikroskopije, a donja slika pomoću RICM.
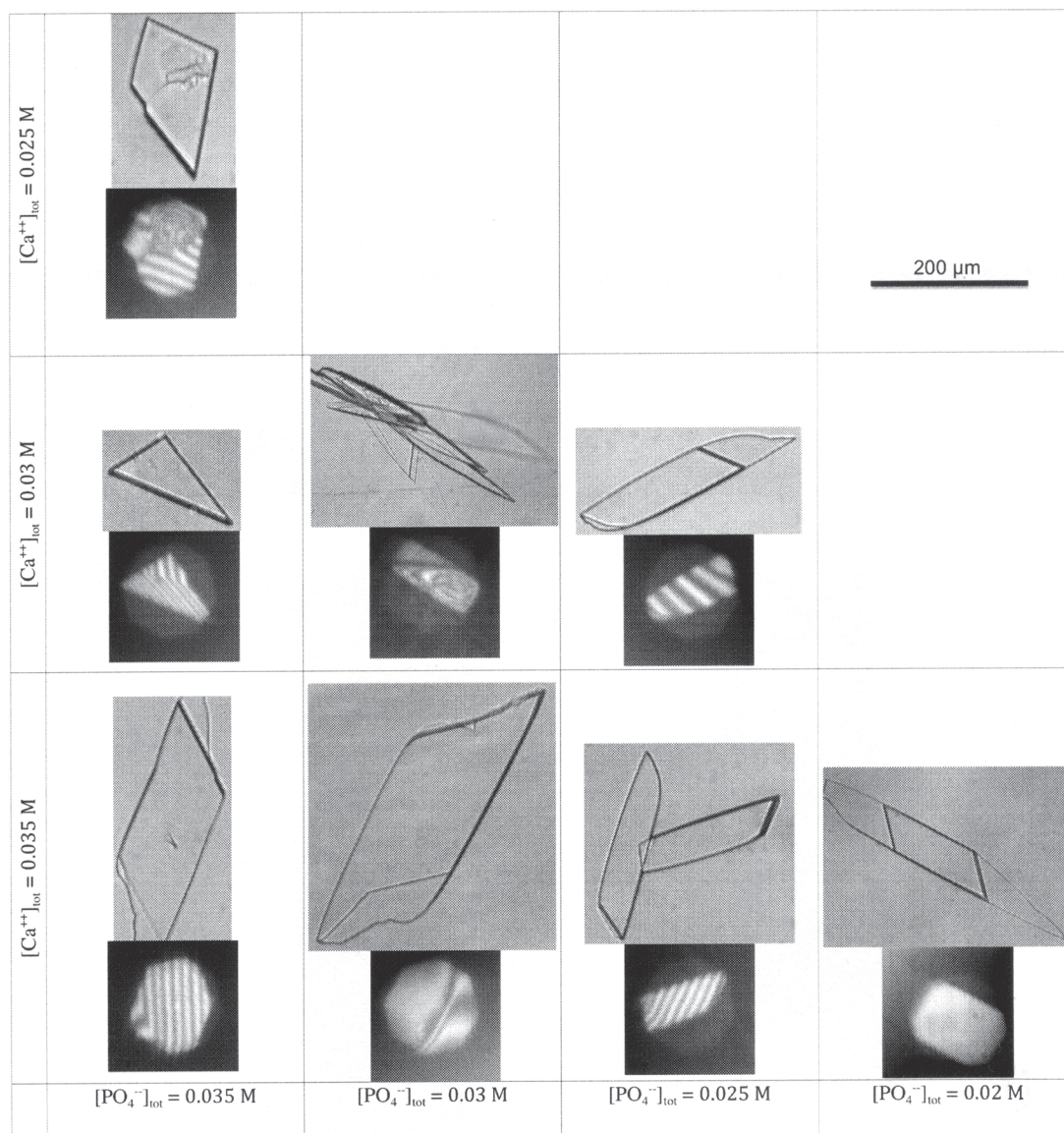
those DCPD crystals nucleated on some surface defects on OTS-treated silica and that those defects were smaller than the optical resolution of the RICM technique. The untreated silica substrate showed the least number of crystals with defined attachment planes. This substrate had the highest surface energy of the three substrates used and yet, the DCPD nucleation did not results in well-defined crystal-substrate contact regions. The intermediate conclusion is that in the case of untreated silica and OTS-modified silica, their surfaces lowered the nucleation enenergy barrier enough to nucleate crystal but the nucleation did not results in any epitaxial growth or different crystal morphology. In the case of albumin coated OTS silica, the energetic barrier for the surface nucleation was not overcome, as no crystal nucleated on this substrate.

The differences between the nucleation of DPCD crystals on two negatively charged surfaces (MTS-treated silica vs. untreated silica) must originate from the chemical differences between the two substrates. The major difference between the two substrates is that UV-oxidized MTS-treated silica surface contains solution-exposed, negatively charged sulfonate groups, while untreated clean silica presents its silanol moieties that are also negatively charged. It has been shown that sulfate groups on surface-attached polysaccharides concentrate calcium ions at interface and thus create local supersaturation necessary for nucleation of calcite [15]. Similar effect on calcite nucleation has also been observed by non-polar polystyrene substrate *after* it was sulfonated by treatment with strong H_2SO_4 acid [16]. We infer that the sulfonate groups on

FIGURE 5.
DPCD crystals grown after 24 hours on OTS-treated silica from solutions of [Ca++]tot and [PO4--]tot as indicated. For each pair of [Ca++]tot and [PO4--]tot concentrations the upper panel shows the bright field image and the lower panel the corresponding RICM image.

SLIKA 5.
Kristal DCPD na siliki modificiranoj s OTS nakon 24h rasta iz otopina $[Ca^{++}]_{tot}$ i $[PO_4^{--}]_{tot}$ kako je naznačeno. Za svaki par koncentracija $[Ca^{++}]_{tot}$ i $[PO_4^{--}]_{tot}$ gornja slika je dobivena pomoću obične mikroskopije, a donja slika pomoću RICM.
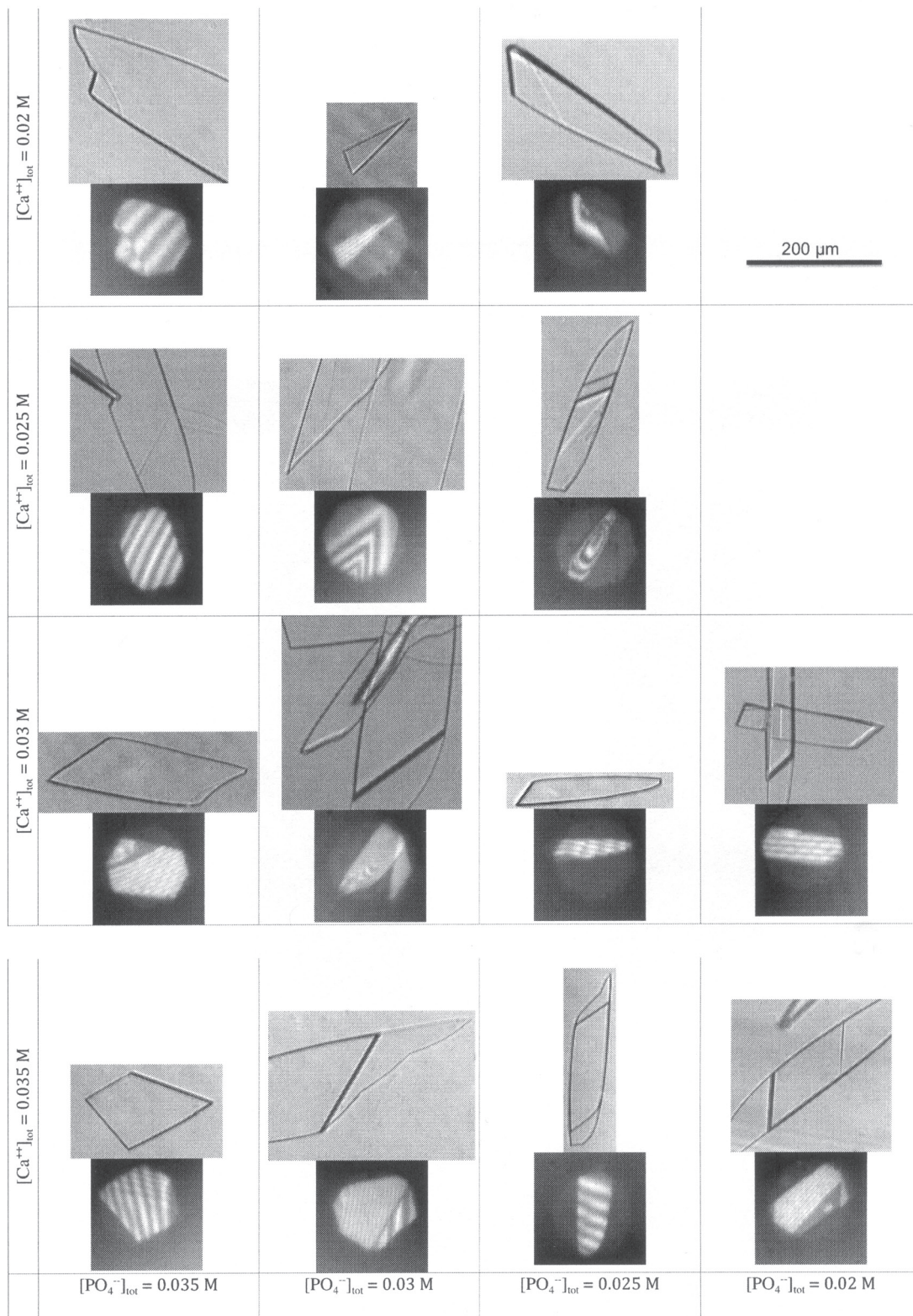
FIGURE 6.
DPCD crystals grown after 24 hours on MTS-treated silica from solutions of [Ca++]tot and [PO4--]tot as indicated. For each pair of [Ca++]tot and [PO4--]tot concentrations the upper panel shows the bright field image and the lower panel the corresponding RICM image.
SLIKA 6.
Kristal DCPD na siliki modificiranoj s MTS nakon 24h rasta iz otopina $[Ca^{++}]_{tot}$ i $[PO_4^-]_{tot}$, kako je naznačeno. Za svaki par koncentracija $[Ca^{++}]_{tot}$ i $[PO_4^-]_{tot}$ gornja slika dobivena je pomoću obične mikroskopije, a donja slika pomoću RICM.
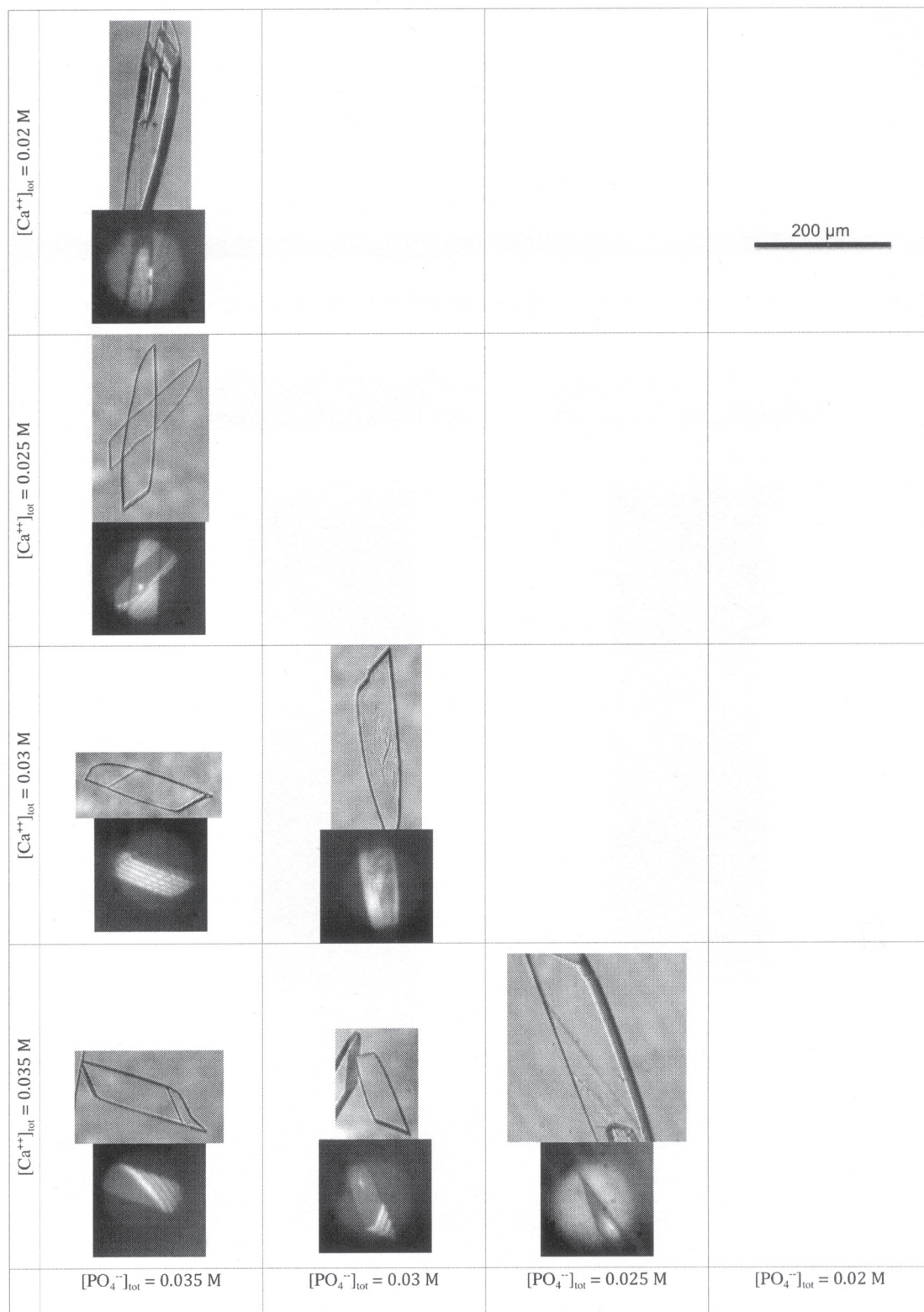
MTS-treated silica acted in a similar fashion by concentrating calcium ions, while the untreated silica substrate with its strongly hydrated silanol groups lacked the same ability to create local calcium supersaturation.

Another possibility for the lack of distinct nucleating planes of DCPD crystals on untreated silica may be due to the specific binding of the phosphate ions to negatively charged silica surface. Phosphate ions can form strong hydrogen-bonded complexes with the silanols of the silica surface with stabilization energies of ~14 kcal/mol per hydrogen bond [17]. Although concentrated by specific binding to silica surface, these bound phosphate ions might have lacked the ability to nucleate DPCD, possibly because of the specific geometry of their bound state.

CONCLUSIONS

Majority of the DCDP crystals grown on different silica substrates appeared to be morphologically similar irrespective of the nature of the nucleating substrate indicating that the surfaces acted by lowering the energy barrier for nucleation of crystals. The exception was found in the case of HSA-treated OTS-silica on which no crystals have nucleated. The RICM provided a proof that the majority of the crystals deposited on substrates were actually not in an extended contact with the substrate surfaces. The inspection of RICM images showed that the contact plane between the crystals and the substrates was at best only a fraction of the projected crystal area (MTS-treated silica), and that in the case of untreated silica the contact planes were absent and the contact was very limited, local and tenuous. These findings were further supported by frequent detachment of the larger crystals from the substrates at longer growth times due to gravity. The crystals nucleated on OTS-treated silica surfaces showed very few well-developed contact planes. Further studies will be necessary to elucidate the kinetics of DCPD crystal nucleation and growth.

REFERENCES

1. Mutaftschiev B. The atomistic nature of crystal growth. Berlin: Springer Verlag; 2001.

2. Kashchiev D. Nucleation: basic theory with applications, Oxford: Butterworth Heinemann; 2000.

3. Boistelle R. Fundamentals of nucleation and crystal growth, In: Garty N, Sato K, editors. Crystallization and polymorphism of fats and fatty acids. New York: Marcel Dekker; 1988.

4. Hlady V, Füredi-Milhofer H. Adsorption of human serum albumin on precipitated hydroxyapatite. J Colloid Interface Sci. 1979;69:460-8.

5. Füredi-Milhofer H, Hlady V, Baker FS, Beebe RA, Wolejko-Wikholm N, Kittelberger JS. Temperature-programmed dehydration of hydroxyapatite. J Colloid Interface Sci. 1979;70:1-9.

6. Brecevic Lj, Hlady V, Füredi-Milhofer H. Influence of gelatin on the precipitation of amorphous calcium phosphate. Colloids Surf. 1987;28:301-13.

7. Komunjer Lj, Marković M, Füredi-Milhofer H. Influence of amino acids on the precipitation kinetics of calcium oxalate monohydrate. J Crystal Growth. 1993;132:122-8.

8. Chow LC, Brown WE. Formation of CaHPO$_4\cdot$2H$_2$O in tooth enamel as an intermediate product in topical fluoride treatments. J Dent Res. 1975;54:65 - 76.

9. Francis MD, Webb NC. Hydroxyapatite formation from a hydrated calcium monohydrogen phosphate precursor. Calcif Tissue Res. 1971;6:355-42.

10. Young RA, Brown WE. Structures of biological minerals. In: Nancollas GH, editor. Biological mineralization and demineralization. Berlin: Springer Verlag; 1982. p. 243-57.

11. Lin YS, Hlady V. Human serum albumin adsorption onto octadecyldimethylsilyl-silica gradient surface. Colloids Surf B Biointerfaces. 1994;2:481-91.

12. Liu J, Hlady V. Chemical pattern on silica surface prepared by UV irradiation of 3-mercaptopropyltriethoxy silane layer: Surface characterization and fibrinogen adsorption. Colloids Surf B Biointerfaces. 1996;8:25-37.

13. Rädler J, Sackmann E. Imaging optical thicknesses and separation distances of phospholipid vesicles at solid surfaces. J Phys II. 1993;3:727-48.

14. Stuart JK, Hlady V. Reflection interference contrast microscopy combined with scanning force microscopy verifies the nature of protein-ligand interaction force measurements. Biophys J. 1999;76:500-8.

15. Addadi L, Weiner S. Interactions between acidic proteins and crystals: Stereochemical requirements in biomineralization. Proc Natl Acad Sci USA. 1985;82:4110-4.

16. Addadi L, Moradian J, Shay E, Maroudas NG, Weiner S. A chemical model for the cooperation of sulfates and carboxylates in calcite crystal nucleation: Relevance to biomineralization. Proc Natl Acad Sci USA. 1987;84:2732-6.

17. Murashov VV, Leszczynski J. Adsorption of the phosphate groups on silica hydroxyls: an ab initio study. J Phys Chem A. 1999;103:1228-38.

HETEROGENA NUKLEACIJA DIKALCIJEVOGA FOSFAT DIHIDRATA NA MODIFICIRANIM POVRŠINAMA SILIKE

Carrie Miller[1], Ljepša Komunjer[2], Vladimir Hlady[1]*

[1]Odjeli za bioinženjerstvo i inženjerstvo i znanost materijala, Sveučilište u Utahu, Salt Lake City, Utah, SAD
[2]Odjel za inženjerstvo industrijskih procesa, Tehnološko sveučilište Compiègne, Compiègne, Francuska
Dopisivanje:
*Prof. Vladimir Hlady
Department of Bioengineering, University of Utah, Salt Lake City, Utah, USA
Email : vladimir.hlady@utah.edu

Izvorni znanstveni rad

SAŽETAK

Istraživana je heterogena nukleacija dikalcijevoga fosfat dihidrata, $CaHPO_4 \cdot 2H_2O$ (DCPD) na ravnoj površini silike te na tri silike s modificiranim površinama: oktadecilsilil (OTS) modificirana silika, OTS silika presvučena s albuminom iz ljudskoga seruma i silika modificirana s 3-merkaptopropiltrietoksisilanom koji je oksidiran pomoću UV zračenja. Omjer prezasićenja otopina kalcija i fosfata, u odnosu na DCPD, bio je manji od 10. Nukleirani kristali promatrani su 24 sata i jedan tjedan poslije inicijalnoga kontakta prezasićenih otopina i površine supstrata pomoću običnoga svjetlosnoga i interferencijski reflektirajućega kontrastnog mikroskopa. DCPD kristali nisu nukleirali na albuminom presvučenoj OTS siliki. Glavnina DCPD kristala, nastala na površini ostalih obrađenih silika, pojavljuje se u morfološki sličnom obliku, bez obzira na kompoziciju površine supstrata. Interferencijsko reflektirajući mikroskop pružio je dokaz da glavnina kristala izrasla na tim supstratima nije stvorila značajan kontakt s površinom supstrata. Slike pokazuju da su se plohe s najopsežnijim kontaktom razvile u slučaju DCPD kristala izraslih na površini silike modificirane s MTS. Kristali koji su nukleirali na OTS modificiranoj siliki pokazali su vrlo mali broj razvijenih kontaktnih ploha.

Ključne riječi: Kalcijev fosfat; Dikalcijev fosfat dihidrat; Teorija heterogene nukleacije; Mikroskop – instrumentacija, metode; Mikroskop – reflektirajući interferencijski kontrastni